DOI:10.28974/idojaras.2025.4.3

IDŐJÁRÁS

Quarterly Journal of the HungaroMet Hungarian Meteorological Service
Vol. 129, No. 4, October – December, 2025, pp. 419–442

Analysis of lower tropospheric temperature trends in the Northern Hemisphere (1940-2023)

Seyed Hossein Mirmousavi * and **Helaleh Fahimi**

Department of Climatology, Faculty of Human Sciences,
University of Zanjan, Zanjan, Iran

**Corresponding author E-mail: hossein.mirmousavi@znu.ac.ir*

(Manuscript received in final form January 12, 2025)

Abstact— This study analyzes long-term (1940–2023) monthly temperature trends across the Northern Hemisphere, focusing on tropical, temperate, and polar regions, as well as key mountainous areas such as the Rocky Mountains, the Tibetan Plateau, and the Alps. Results show that polar regions experienced the highest seasonal temperature increase, averaging 0.081°C per season during winter, while tropical regions exhibited the lowest increase, with 0.036°C during winter. In temperate regions, seasonal warming trends ranged from 0.05°C in winter to 0.039°C in summer. Monthly trends revealed that February and March exhibited the highest increases, with rates of 0.0195 °C and 0.0194 °C, respectively, while August showed the lowest increase at 0.0116 °C. Furthermore, trend maps indicate that over 92% of the Northern Hemisphere experienced warming across all months except June and January. These findings provide a comprehensive understanding of regional and seasonal temperature variations in the Northern Hemisphere, emphasizing the importance of localized and temporal analyses for a more nuanced perspective on climate change.

Key-words: Northern Hemisphere, temperature trend, lower troposphere, Intertropical Convergence Zone

1. Introduction

Air temperature is a fundamental driver of surface-atmospheric processes, influencing weather, climate, and ecological systems (*Vinniko et al*., 1990). Over recent decades, the rise in global temperatures has been well-documented across all latitudes and seasons (*Simmons et al*., 2017; *Hansen et al.*, 2010; *Al Mutairi et al*., 2023). However, these changes are neither uniform across time and space nor consistent in magnitude, with some regions experiencing accelerated warming

while others exhibit minimal change or even cooling trends (*Luterbacher et al*., 2005; *Siddik* and *Rahman*, 2014).

Since the late 19th century, significant warming has been observed, particularly during the periods of 1920–1944 and post-1975 (*Jones* and *Moberg*, 2003). Research suggests that warming in the Northern Hemisphere has been approximately double that of the Southern Hemisphere, with the most pronounced trends occurring in higher latitudes (*Croitoru et al*., 2012; *Steiner et al*., 2020). This hemispheric disparity can be attributed to factors such as reduced sea ice thickness in polar regions, which intensifies heat conduction to the surface, especially during colder months (*Manabe* and *Stouffer,* 1979, 1980). Conversely, summer warming in Arctic regions is moderated by seasonal sea ice loss (*Manabe* and *Stouffer,* 1979). Seasonal variations in warming trends are further corroborated by studies like *Chapman* and *Walsh* (1993), who identified distinct increases in winter and spring temperatures, while summer trends remained negligible. Although the magnitude of these increases varies across studies due to differences in datasets and methods, there is broad agreement on the accelerated warming since the mid-20th century (*Folland et al*., 2001; IPCC, 2013). Recent findings highlight an average warming of 0.06 °C per decade since 1850, with this rate tripling since 1982 (*Lindsay*, 2005). The primary driver of this warming is the increased concentration of greenhouse gases, predominantly from anthropogenic activities (*Choi et al*., 2009; *Trewin,* 2016). Beyond surface temperatures, tropospheric warming patterns provide additional insights, with observations indicating a warming rate of 0.14 °C per decade since 1958 (*Lindzen et al*., 2002). However, variations in warming rates between the surface and the troposphere, as well as across geographic regions, highlight the complexity of these processes (*Christy et al.*, 2007). The impacts of global warming are profound, including reduced snow and ice cover (*Rosenzweig et al.*, 2008), increased frequency of extreme weather events (*Reidmiller et al*., 2018), and shifts in precipitation patterns leading to more floods and droughts (*Salzmann*, 2016; *Tabari*, 2020). While these phenomena have been extensively studied at global scales, there are notable gaps in regional and long-term analyses. Research has disproportionately focused on short-term trends and neglected the detailed examination of specific geographic regions, such as mountainous areas or distinct latitudinal zones.

This study addresses these gaps by conducting a comprehensive monthly and long-term analysis (1940–2023) of temperature trends in the Northern Hemisphere. It focuses on key mountainous regions, including the Rockies, Appalachians, Himalayas, Alps, and the Tibetan Plateau, while also examining trends across tropical, temperate, and polar zones. By distinguishing trends by geographic region and season, this research aims to provide a detailed understanding of regional and temporal variations, contributing to the broader discourse on climate change and its localized impacts.

2. Data and methodology

Monthly temperature data were extracted from the ERA5 dataset provided by the ECMWF database for the statistical period of 1940–2023. ERA5 data have been available since 1940, which is why the start of the statistical period in this study is set from that year. The temperature trend analysis was conducted at the 850 hPa pressure level. The 850 hPa level is one of the most commonly used atmospheric levels. The 850, 925, and 1000 hPa pressure levels are nearly similar to sea-level pressure maps (Rahimi 2010). Thus, the selection of the 850 hPa level as a lower tropospheric layer can simultaneously provide valuable information regarding both the earth's surface and the 1000 hPa level. Since most of the regions examined in this study have elevations exceeding sea level, it is likely that the 1000 hPa level and sea level data may not be suitable for areas with elevations above 100 meters, and the results might not align with actual conditions. Moreover, at the 850 hPa level, the topography's influence on climatic parameters is better represented. For this reason, the 850 hPa level was deemed more appropriate for analyzing lower tropospheric temperature trends in this research. Given that the primary objective of this study is to examine temperature trends in the Northern Hemisphere, the study area encompasses latitudes from 0 to 90 degrees north and longitudes from 180 degrees west to 180 degrees east. For a more detailed analysis, the tropical region was defined as latitudes from 0 to 30 degrees north, the temperate zone as latitudes from 30 to 60 degrees north, and the polar region as latitudes from 60 to 90 degrees north (*Fig. 1*).

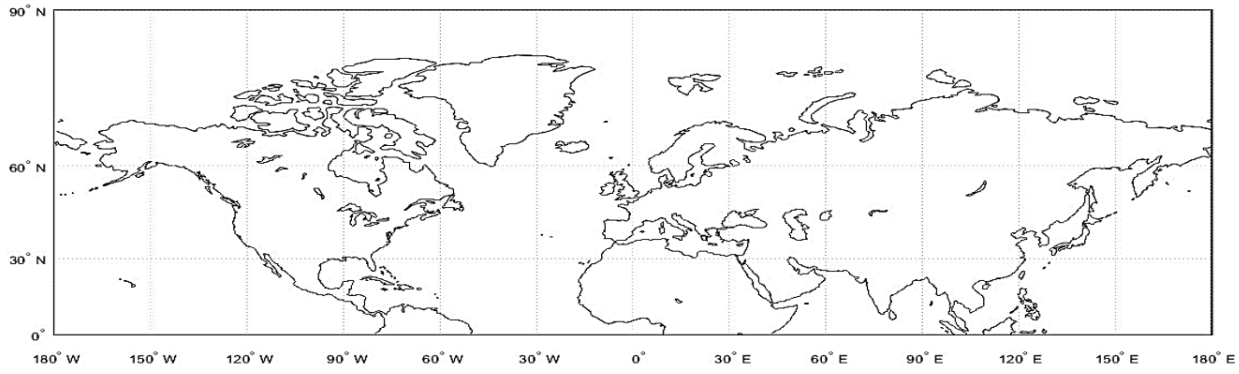

Fig. 1. The study area.

In order to check the normality of data distribution, the Q-Q and P-P graphicalmethods were used. Graphical methods can perform better than quantitative methods due to the fact that they are able to show the location and cause of the lack of goodness of fit in the total data (*Asakereh*, 2011).

2.1. Q-Q plot (quantile-quantile diagram)

The Q-Q plot (quantile-quantile plot) is a graphical tool used to compare the quantiles of observed data with those of a theoretical distribution, such as a normal distribution, to assess data normality. If the points form a straight line, it indicates that the data conforms to the theoretical distribution. The coordinates of the points of this diagram show the position of the points whose coordinates are obtained from real and theoretical estimations and measurements. To draw the Q-Q graph, first, the observations are arranged in ascending order from 1 to *n* (*n* is the number of observations) and drawn along the x-axis. On the y-axis, the expected quantile points, which are a function of the rank and length of the statistical period, are plotted. This axis has a cumulative distribution function equal to and less than observation (*Asakereh*, 2011).

2.2. P-P plot (probability-probability diagram)

The P-P plot (Probability-Probability plot) evaluates the cumulative probability of observed data against expected probabilities, providing another method to test normality. In a P-P plot, the cumulative probability of the observed data is plotted against the cumulative probability of the expected values from the assumed distribution. If the points fall on the 45-degree line (the bisector), it suggests that the observations fit the assumed distribution well. In the case of normality, the cumulative probability in a normal distribution is defined by the equation:

$$F_m = \left(Z \leq \frac{x_m - \overline{x}}{s_m}\right) \quad , \tag{1}$$

where F_m is the cumulative probability associated with the m-th ordered observation, x_m denotes the m-th order statistic (the m-th smallest value in the sample), $\overline{x}$ is the sample mean, s_m represents the estimated standard deviation corresponding to the m-th ordered value, Z is a standard normal random variable with distribution N(0,1), P ($Z \leq \cdot$) refers to the cumulative distribution function (CDF) of the standard normal distribution. Plotting the values of Fm against m/n produces the P–P plot. The deviation between Fm and m/n indicates the extent to which the empirical distribution departs from normality. In the P–P plot, the x-axis represents the empirical probability values (m/n), while the y-axis represents the expected probability values from the normal distribution (*Asakereh, 2011*). To further clarify the statistical methodologies employed, we emphasize that the P-P plot assesses the goodness-of-fit of observed data against a theoretical distribution by comparing cumulative probabilities. The Q-Q plot, in contrast, examines whether the distribution of data follows the theoretical quantiles. These graphical methods, combined with the Kolmogorov-Smirnov test, ensure the robustness of the assumption of normality (*Neter et al*., 1988). Additionally, the selection of the least squares regression method was based on its effectiveness in reducing errors

while analyzing long-term trends in climatic datasets *(Asakereh, 2011; Momeni, 2008)*. Further validation was achieved through reanalysis of key datasets such as ERA5 from previous studies (*Simmons et al., 2017*), ensuring consistency with established methodologies.

2.3. Least squares method

The least squares regression line is the one that minimizes the sum of the squared vertical distances between the observations *Y* and the line (*Neter et al*. 1988). In other words, it fits a line to the data in such a way that the sum of squared errors is minimized (*Asakereh*, 2011). The simple linear regression model was estimated using the least-squares method. In this approach, the intercept and slope of the fitted regression line are denoted by b_0 and b_1, respectively. The least-squares criterion requires that b_0 and b_1 minimize the function Q, defined as the sum of the squared deviations between the observed values and the fitted values:

$$Q = \sum_{i=1}^{n} [Y_i - (b_0 + b_1 x_1)]^2 \, . \tag{2}$$

In the simple linear regression model, the least squares estimators for b_0 and b_1 are given by the following formulas:

$$b_1 = \frac{\sum X_1 Y_1 - \frac{(\sum X_1)(\sum Y_1)}{11}}{\sum X_1^2 - \frac{(\sum X_1)^2}{11}} \, , \tag{3}$$

$$b_0 = \frac{1}{n} (\sum Y_1 - b_1 \sum X_1) \, , \tag{4}$$

Therefore, the least squares estimates b_0 and b_1 are obtained by calculating the values of $\sum X_1$,$\sum Y_1$, $\sum X_1 Y_1$, and $\sum X_1^2$ from the sample data and substituting them into Eqs. (3) and (4) (*Neter et al*., 1988).

2.4. Significance level

Significance refers to the probability of making an error when rejecting the null hypothesis H_0. It is also known as the p-value. The smaller the significance value, the easier is to reject the null hypothesis. The critical region probability of the sampling distribution (α) is the level of error that the researcher is willing to accept (*Momeni*, 2007). Thus, in a statistical test, the null hypothesis H0 is either rejected or accepted against the alternative hypothesis H1 with an error probability of alpha (*Asakereh*, 2011). By choosing the significance level, α determines the acceptable probability of error.

$$\text{Sig} \; < \alpha \rightarrow \; H_0 \text{ is rejected} \tag{5}$$

$$\text{Sig} \geq \alpha \rightarrow H_0 \text{ is accepted} \quad (6)$$

In this study, the temperature trend was analyzed with a 95% significance level and an error rate of 0.05.

3. Discussion and conclusion

To select an appropriate method for analyzing temperature trends, the normality of the data was first tested. Although it is generally assumed that long-term data follow a normal distribution, graphical methods such as P-P and Q-Q plots were used to ensure greater accuracy, confirming the normality of the data. Following the confirmation of normality, a parametric linear regression method based on the least squares criterion with a 95% significance level was applied to determine the temperature trends (*Neter et al*., 1988). Temperature trend maps for each month across the Northern Hemisphere were generated, and the interpretation of these maps is presented below. This study analyzed the percentage of areas experiencing increasing and decreasing temperature trends, as well as the magnitude of these trends on a monthly and seasonal basis across three regions: the tropical, temperate, and polar zones. Special attention was given to cold regions and high-altitude areas during the statistical period of 1940 to 2023. The resulting temperature trend maps indicate that increasing temperature trends dominate throughout all months in the Northern Hemisphere. However, regional differences in the magnitude of warming are clearly observed during monthly and seasonal intervals (*Feidas et al*., 2005). Except for the months of June (covering 86% of the area) and January (covering 89% of the area), more than 92% of the Northern Hemisphere experienced increasing temperature trends in the remaining months. One of the most obvious early signs of climate change is the warming of air and oceans, as well as the melting of land ice and polar ice (*Seidel et al.,* 2018). This phenomenon is strongly reflected in the findings of the present study. Cold regions of the Northern Hemisphere, including the polar regions, Greenland, Alaska, Siberia, the Tibetan Plateau, and high-altitude areas such as the Himalayas and the Alps, have experienced significant temperature increases. Some regions, such as Alaska, Siberia, and the Tibetan Plateau, have even emerged as hotspots of warming. This result is consistent with *Huang et al.* (2023) study, which showed that between 1991 and 2019, the spatial extent of cold areas decreased by 7.13% compared to the period of 1901 to 1930.

3.1. Seasonal temperature trends in the Northern Hemisphere

The largest area with a positive temperature trend in the Northern Hemisphere is observed during the autumn season (*Table 1 Fig.2.* B), with an increase of 0.042 °C. Following autumn, the seasons of spring, winter, and summer,

respectively, have the largest areas with increasing temperature trends. Although summer is typically the warmest season, it shows a higher percentage of areas with decreasing trends compared to other seasons. In winter, while the area with an increasing trend is smaller compared to autumn and spring, the highest rate of temperature increase is recorded during this season. These findings align with multiple studies which demonstrated that winter temperature increases are more pronounced than in other seasons. Examples include the works of *Karl et al.* (1993), *Otterman et al.* (2002). This temperature increase has also been observed regionally. For instance, more pronounced warming in winter has been reported in regions such as Saudi Arabia (*Almazroui,* 2020), Korea (*Chung* and *Yoon*, 2000), the mid-latitudes of Asia (IPCC, 2014), and Venezuela and Colombia (*Quintana-Gomez*, 1999). The lowest temperature trend is observed in the summer season (*Table 1, Fig. 2.* A), meaning that summer not only has the smallest area with a positive trend, but also shows the lowest increase in temperature. In terms of decreasing trends, winter exhibits the largest negative trend, while spring shows the smallest (*Table 1* and *Fig. 2.* A).

Table 1. Percentage of the area and the amount of decreasing and increasing trends of the Northern Hemisphere in different seasons of the year during the statistical period of 1940–2023

Seasons	Area with negative trend (%)	Magnitude of negative trend	Area with positive trend (%)	Magnitude of positive trend
Winter	7.41	-0.021	92.57	0.056
Spring	7.20	-0.014	92.79	0.045
Summer	8.26	-0.017	91.73	0.038
Autumn	4.05	-0.016	93.75	0.042

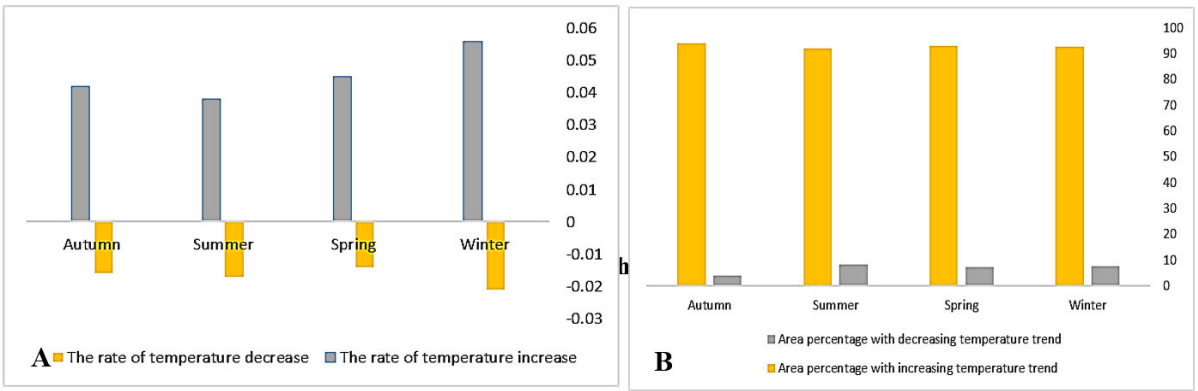

Fig. 2. Seasonal analysis of temperature trends: magnitude and spatial coverage (1940–2023)

3.2. Monthly temperature trends in the Northern Hemisphere

Given the varying results for the negative temperature trends across different months, it is difficult to attribute the decline in negative trends specifically to the warmer or colder months of the year. However, for the positive temperature trends, the opposite is true. The rate of increase in positive trends is higher in the colder months compared to the warmer ones (*Table 2, Fig. 3*). February and March exhibit the highest positive temperature trends and the lowest negative trends (*Figs. 3–5, Table 2*). After February and March, the highest temperature increases occur in December, January, and November (*Figs. 3* and *4, Table 2*).

Table 2. Monthly temperature trends in the Northern Hemisphere (1940–2023): area coverage and magnitude of increasing and decreasing trends

Month	Percentage of area with positive trend (%)	Change per year	Percentage of area with significant positive trend (%)	Percentage of area with negative trend (%)	Change per year	Percentage of area with significant negative trend (%)
December	96.10	0.0175	55.11	3.89	-0.0037	0.0021
January	89.02	0.0193	57.80	10.97	-0.0057	0.0200
February	92.62	0.0195	52.80	7.37	-0.0119	0.5200
March	89.63	0.0194	58.95	10.37	-0.0073	0.9500
April	97.25	0.0140	47.53	2.74	-0.0031	0.0023
May	91.50	0.0120	48.00	8.49	-0.0043	0.8700
June	86.57	0.0130	55.50	13.42	-0.0069	1.5700
July	94.02	0.0140	67.31	5.98	-0.0054	0.4200
August	94.62	0.0116	56.32	5.38	-0.0047	0.6000
September	93.55	0.0130	60.60	6.44	-0.0052	0.2400
October	92.23	0.0120	49.85	7.76	-0.0073	0.0660
November	95.48	0.0170	55.10	4.51	-0.0035	0.0000

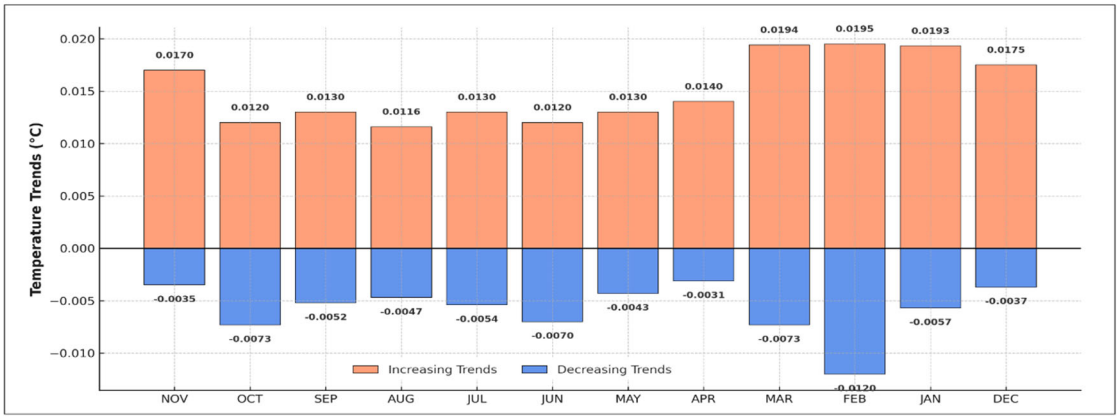

Fig. 3. Increasing and decreasing trends of the monthly temperature of the Northern Hemisphere during the statistical period (1940-2023)

These findings are further detailed in *Table 2* and illustrated in *Figs. 4,5,8,* and *10,* which show the spatial extent and magnitude of temperature trends across the Northern Hemisphere. For example, *Fig. 5* highlights the warming trends in March and April, particularly in temperate regions, while *Fig. 10* provides insights into the variations observed during autumn months such as October and November.

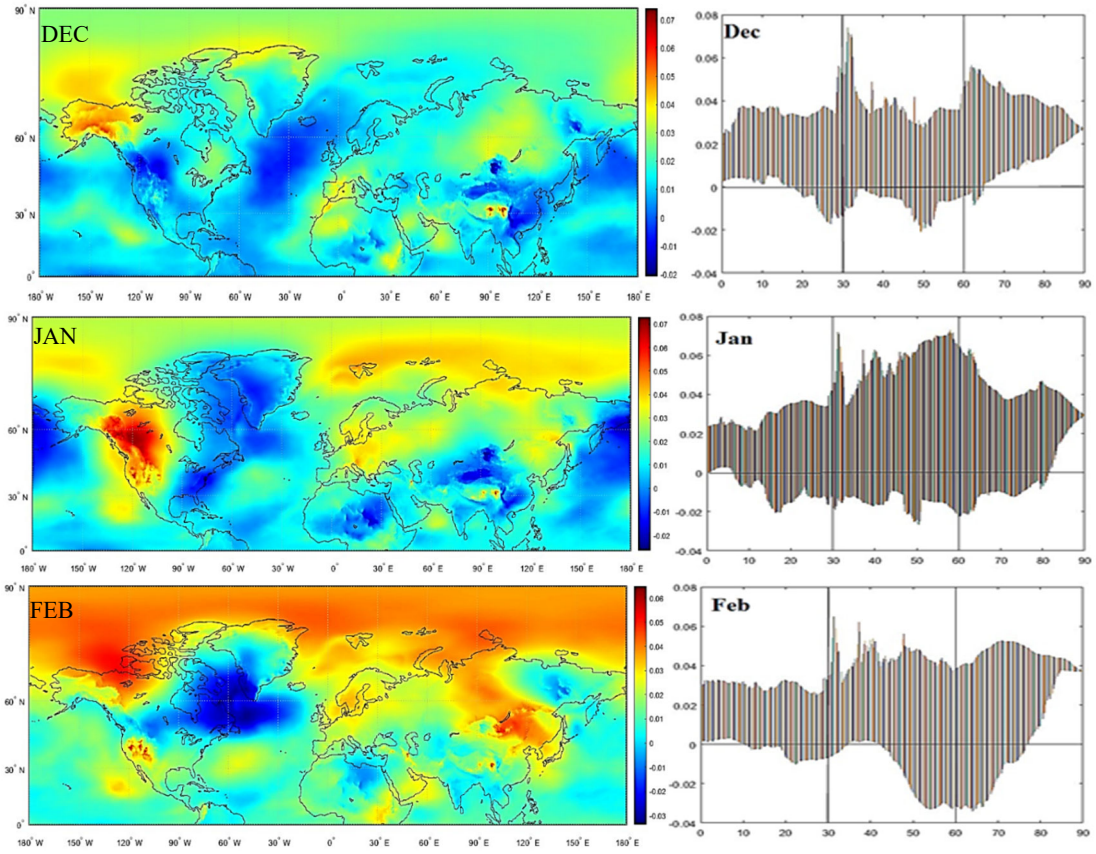

Fig. 4. The temperature trend of the winter months (December, January, February) of the Northern Hemisphere during the statistical period from 1940 to 2023.

The largest temperature increases are observed during the colder months, while the smallest increases are recorded in August, during the summer season. Following August, September and October show similarly small differences in positive temperature trends (*Fig. 10*, A and B), with June and September both exhibiting an increase of 0.013 °C. Furthermore, February and March show the largest temperature decreases in regions with negative trends, with reductions of -0.011 °C and -0.0073 °C, respectively. In terms of area with increasing trends, April covers the largest area, with only 2.74% of the Northern Hemisphere experiencing negative trends in this month. These negative trends are concentrated in regions such as eastern Pakistan, central China in northern Tibet,

the northern Atlantic Ocean, and Canada in North America (*Fig. 5*, B and E). The largest area with negative trends occurs in the warm month of June, covering 13.4% of the Northern Hemisphere, with a temperature decline of -0.0069 °C. Following June, January during the winter season also shows a larger area with negative temperature trends, with a decrease of -0.0057 °C. In June and July, during the summer, more tropical regions experience negative trends (*Fig. 8*, A, B, D, and E). *Table 2* provides the percentage of areas with significant temperature trends.

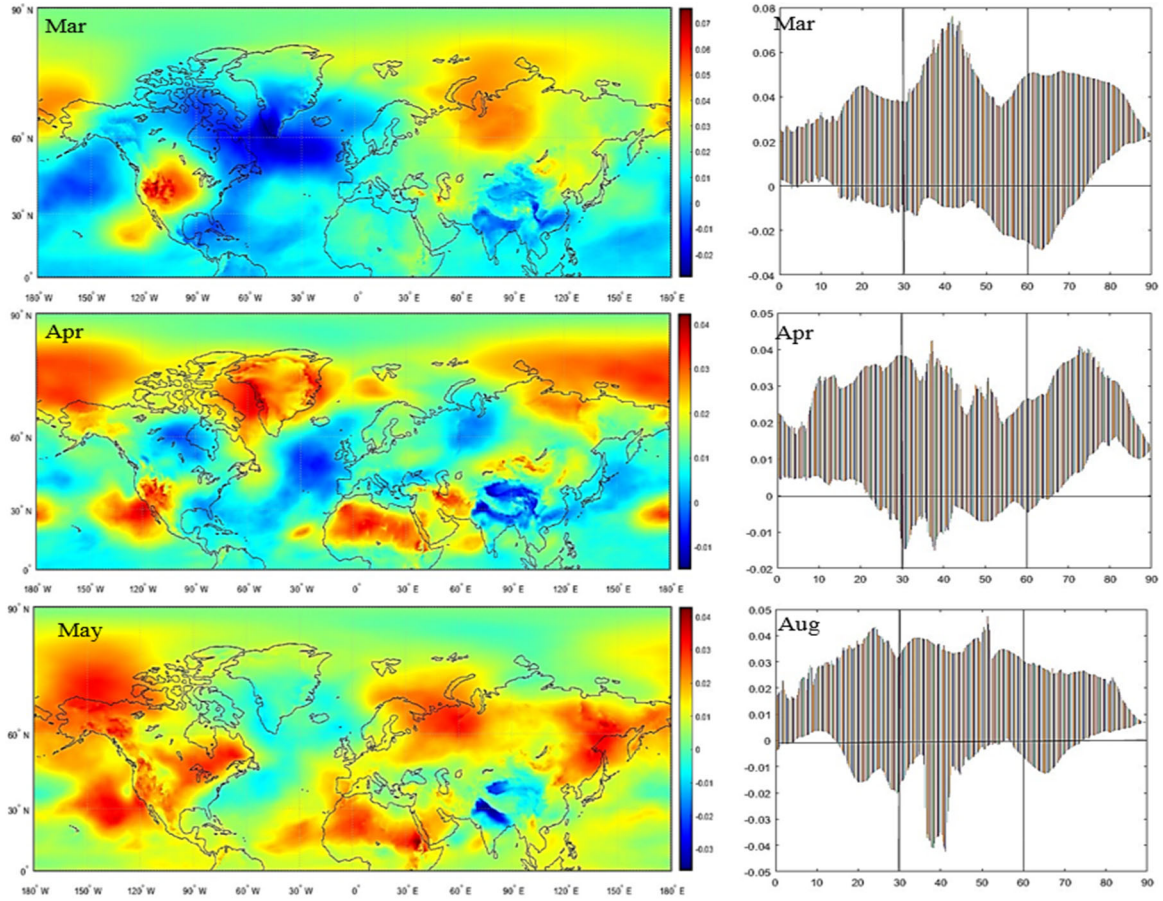

Fig. 5. The temperature trend of the spring months (March, April, May) of the Northern Hemisphere during the statistical period from 1940 to 2023

As shown in *Fig. 5*, the warming trends during March, April, and May are more pronounced in temperate regions, particularly in the transition from winter to spring. These trends indicate the influence of seasonal factors on regional warming.

3.3. Seasonal trends in the tropical, temperate, and polar regions

In all seasons, the positive temperature trend increases progressively from the tropical regions towards the polar regions (*Figs. 5,6,* and *8, Table 3*). In the polar region, winter records the highest positive temperature trend with an increase of 0.018 °C. The months of February, January, March, and December show the highest positive temperature trends in the polar region, all of which are statistically significant. During the cold months, a larger percentage of the polar region experiences a significant temperature trend, while in the tropical region, the area with a significant temperature trend decreases during the cold months. Conversely, during the warm months, the tropical region shows a larger significant area with increasing temperature trends (*Fig. 11*). The temperate regions, on the other hand, exhibit the smallest significant area with temperature trends throughout the year (*Fig. 11*). Spring, summer, and autumn show the highest positive temperature trends in the polar region. In the temperate region, the highest temperature increases during the cold months occur in March, January, February, and December. However, in the tropical region, autumn records the largest temperature increase (*Table 3, Fig. 6*). For the tropical region, it is not possible to clearly rank the months with the highest temperature increases based on cold or warm seasons, as temperature changes in this region are influenced by various factors that do not align strictly with seasonal patterns.

Table 3. Seasonal temperature trend increase rates in the tropical, temperate, and polar regions (1940–2023)

Season	**Polar**	**Temperate**	**Tropical**
Winter	0.081	0.050	0.036
Spring	0.052	0.044	0.024
Summer	0.046	0.039	0.030
Autumn	0.045	0.041	0.037

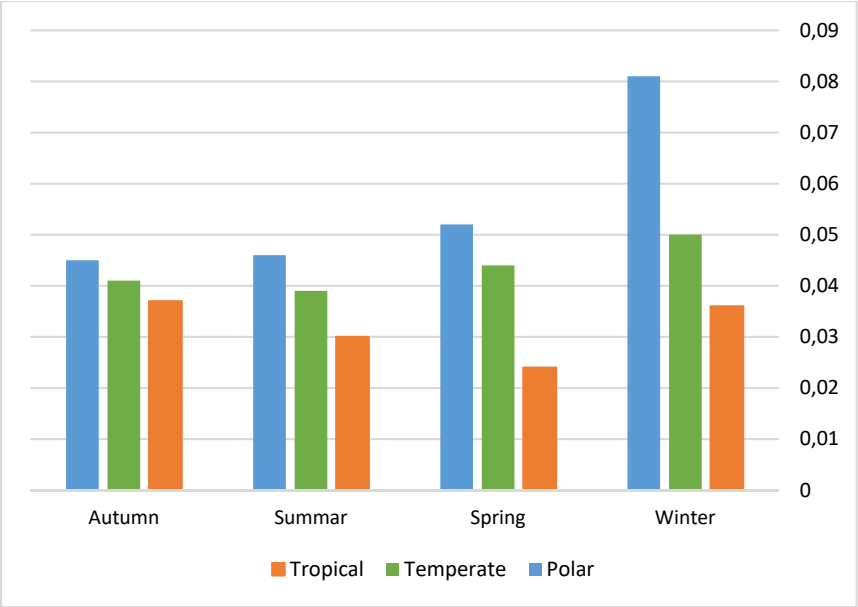

Fig. 6. Seasonal temperature increase rates in tropical, temperate, and polar regions (1940–2023).

3.4. Monthly trends in the tropical, temperate, and polar regions

The monthly temperature trends in tropical, temperate, and polar regions were analyzed separately. According to *Steiner et al*. (2020), the most intense warming occurs in the mid-to-high latitudes of the Northern Hemisphere, with the Arctic warming at twice the global average. However, recent research has shown that even tropical regions are undergoing changes (*Seidel et al*., 2008), although the smallest temperature variations occur in the tropical region (*Manabe et al*., 2011). Compared to the temperate and polar regions, the tropical region has the highest percentage of area with a positive trend and, consequently, the lowest percentage of areas with a negative trend (*Figs. 4–10*, *Tables 4* and *5*). Except for the months of April and October, the warming in the tropical region is lower than in other regions (*Fig. 5*, B, E, *Fig. 10*, B, E; *Fig 7* and *9, Tables 4-5*), which is consistent with previous findings. However, this study revealed that the lower warming trend in the tropical region is mainly confined to latitudes between 0 and 8 degrees north, where the rate of temperature increase is more uniform and lower compared to other regions. This does not apply to other tropical areas between 8 and 30 degrees north. Based on the rate of temperature increase, the tropical region can be divided into two parts: 0 to 8 degrees north and 8 to 30 degrees north. In all months except December, the warming trend in the Intertropical Convergence Zone (ITCZ) region (between 0 and 8 degrees north) is lower than in other tropical regions and other parts of the Northern Hemisphere (*Figs. 4,5,8,* and *10*). In this zone, the rate of temperature increase is consistent, ranging between 0.02 and

0.025 °C. North of 8 degrees, up to 30 degrees, the warming rate increases. The rate of warming in latitudes between 8 and 30 degrees is similar to that of temperate and polar regions (*Figs. 4, 5, 8, and 10*, D, E, F). For instance, in September, the warming rate between 8 and 30 degrees is higher than in the temperate and polar regions (*Fig. 10*, D). Additionally, in October, November, and May, warming hotspots in northern Africa show a greater increase compared to the temperate and polar regions (*Fig. 10*, E, F*; Fig. 5*, C).

Since air temperature is often described as an average (*Tamarin-Brodsky et al.*, 2019), temperature trends represent trends in average temperatures. The average temperature of the tropical region reflects on a combination of lower temperatures in the ITCZ and higher temperatures in latitudes between 8 and 30 degrees. This is why the warming trend in the tropical region is recorded as lower than in other regions. Among all the months of the year, the warming trend in the tropical region during October and April stands out from other months (*Table 4, Fig. 7*, B). In April, the tropical region experiences a higher warming trend compared to temperate regions and equal to that of the polar region (*Fig. 7,* B). In October, the warming trends in the tropical and temperate regions are equal to and higher than in the polar region. In December, temperatures between 0 and 3 degrees north remain around 0.02 °C, but beyond 4 degrees, the temperature increases (*Fig. 7*, B). This explains why the tropical region exhibits its highest warming trend in December compared to other months (*Table 4, Fig. 7*).

Table 4. Percentage of the area and the value of the increasing trend of the Northern Hemisphere in the three tropical, temperate, and polar regions during the statistical period of 1994-2023

Month	Percentage of area with positive trend in the tropics (%)	Rate of positive trend in the tropics	Percentage of area with positive trend in the temperate region (%)	Rate of positive trend in the temperate region	Percentage of area with positive trend in the polar region (%)	Rate of positive trend in the polar region
December	98.93	0.0138	90.30	0.0147	99.18	0.0230
January	95.31	0.0113	80.00	0.1950	91.66	0.0270
February	97.45	0.0110	87.17	0.0160	93.13	0.0310
March	94.89	0.0037	83.21	0.0198	90.67	0.0270
April	98.87	0.0129	93.57	0.0113	99.20	0.0129
May	97.38	0.0048	87.07	0.0136	89.99	0.0125
June	96.58	0.0100	88.08	0.0140	74.94	0.1520
July	97.61	0.0100	91.80	0.0130	92.60	0.0190
August	97.96	0.0103	91.06	0.0124	94.80	0.0123
September	98.28	0.0114	91.80	0.0130	93.80	0.0154
October	98.90	0.0138	84.57	0.0138	92.59	0.0120
November	99.79	0.0124	87.91	0.0145	98.68	0.1800

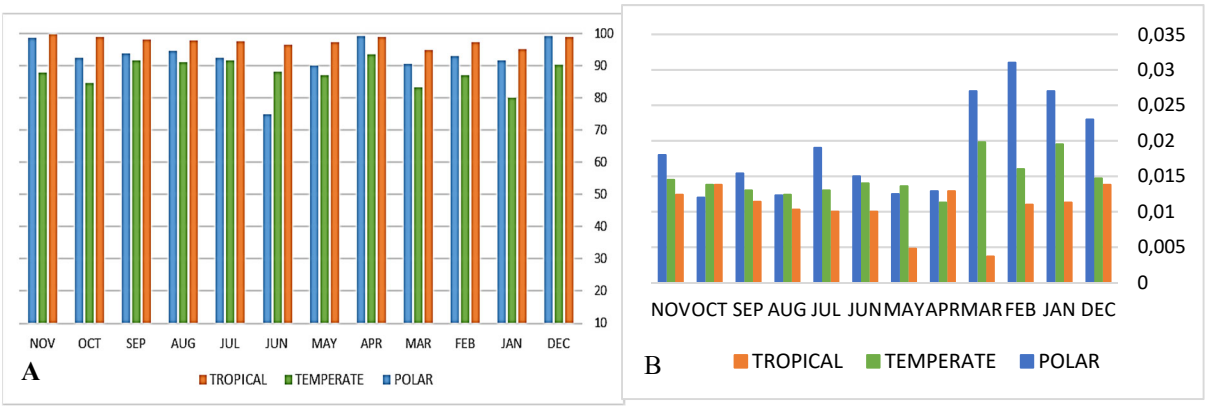

Fig. 7. A - percentage of area with increasing trends; B - magnitude of increasing trends in tropical, temperate, and polar regions (1994–2023).

The temperate region has the largest area with a decreasing trend compared to the tropical and polar regions (*Table 5, Fig. 9*, B). In January, the largest area with a decreasing trend was recorded in the temperate region, which contrasts with the pattern observed in other months (*Fig. 8*, B, E, *Table 5, Fig. 9,* A). This indicates that the area with a decreasing trend in the polar regions has diminished. In June, 25% of the polar region showed a decreasing trend, marking the highest area with a decreasing trend in the polar region compared to other months (*Fig. 8*, A, D). However, the greatest amount of trend reduction was recorded in February (*Table 5, Fig. 9*, A). The tropical region also experienced a decreasing trend, with the highest reduction occurring in June (*Table 5, Fig. 9*, B). The amount of decrease in the tropical, temperate, and polar regions varies across other months and cannot be clearly categorized based on warm or cold months (*Table 5, Fig. 9*).

Table 5. Percentage of the area and the amount of the decreasing trend of the Northern Hemisphere in the tropical, temperate and polar regions during the statistical period of 1994–2023

Month	Percentage of area with negative trend in the tropics (%)	Rate of decreasing trend in the tropics	Percentage of area with negative trend in the mid-latitudes (%)	Rate of decreasing trend in the mid-latitudes	Percentage of area with negative trend in the polar region (%)	Rate of decreasing trend in the polar region
December	1.06	-0.0051	9.86	-0.0037	0.081	-0.0091
January	4.68	-0.0046	19.99	-0.0050	8.230	-0.0059
February	2.54	-0.0030	12.82	-0.0130	6.860	-0.0128
March	5.10	-0.0119	16.78	-0.0083	9.320	-0.0076
April	1.12	-0.0026	6.42	-0.0033	0.700	-0.0015
May	2.62	-0.0010	12.92	-0.0045	10.000	-0.0025
June	3.41	-0.0092	11.91	-0.0049	25.050	-0.0076
July	2.38	-0.0048	8.19	-0.0055	7.370	-0.0054
August	2.03	-0.0061	8.93	-0.0034	5.160	-0.0050
September	1.79	-0.0047	8.19	-0.0055	6.150	-0.0060
October	1.07	-0.0051	15.42	-0.0087	7.400	-0.0040
November	0.20	-0.0018	12.08	-0.0037	1.310	-0.0210

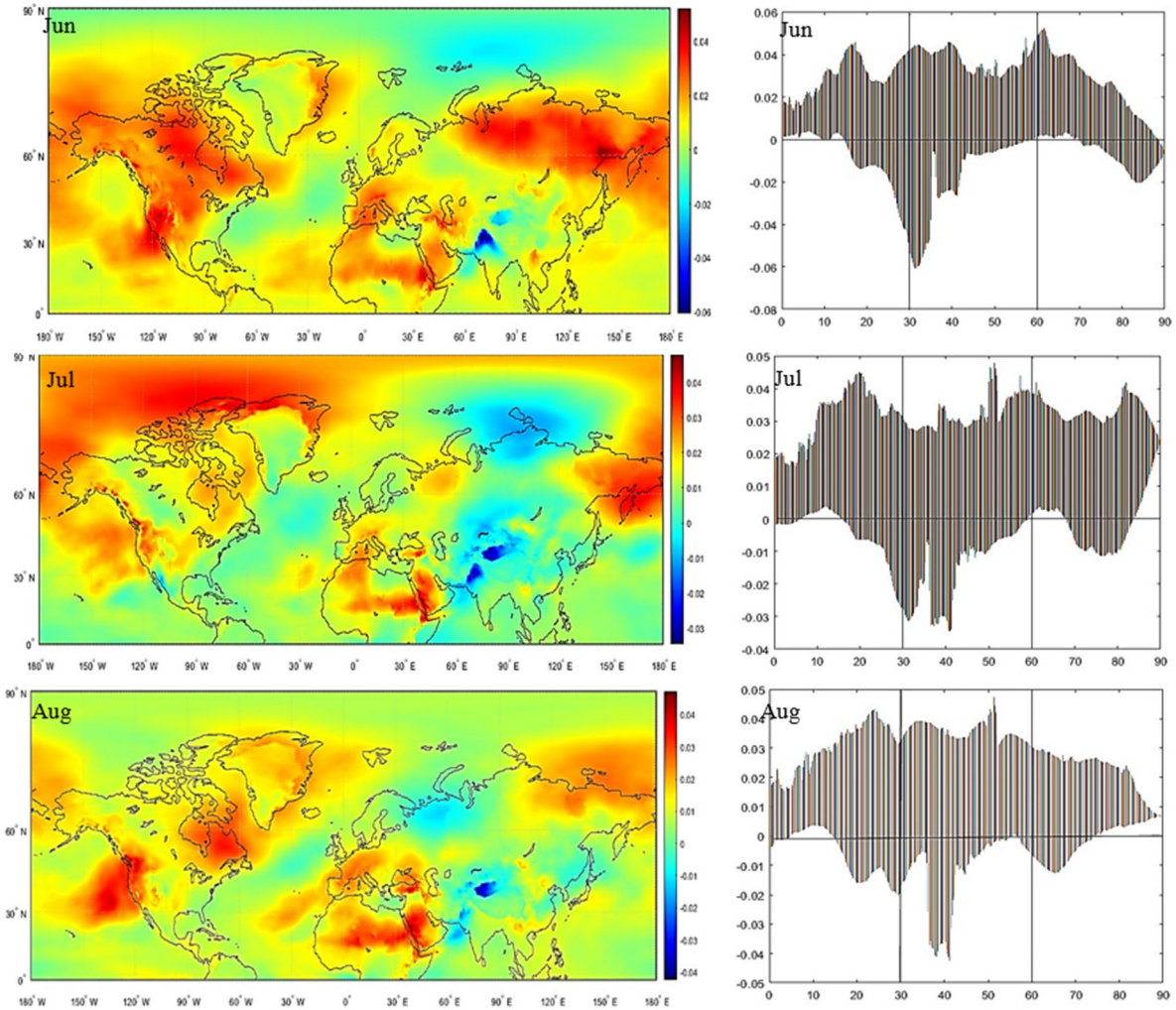

Fig. 8. The temperature trend of the summer months (June, July, August) of the Northern Hemisphere during the statistical period from 1940 to 2023.

Fig. 8 highlights the warming trends during summer months (June, July, August), where the northern temperate regions exhibit the strongest warming compared to tropical areas. This pattern suggests that summer warming is more regionally heterogeneous.

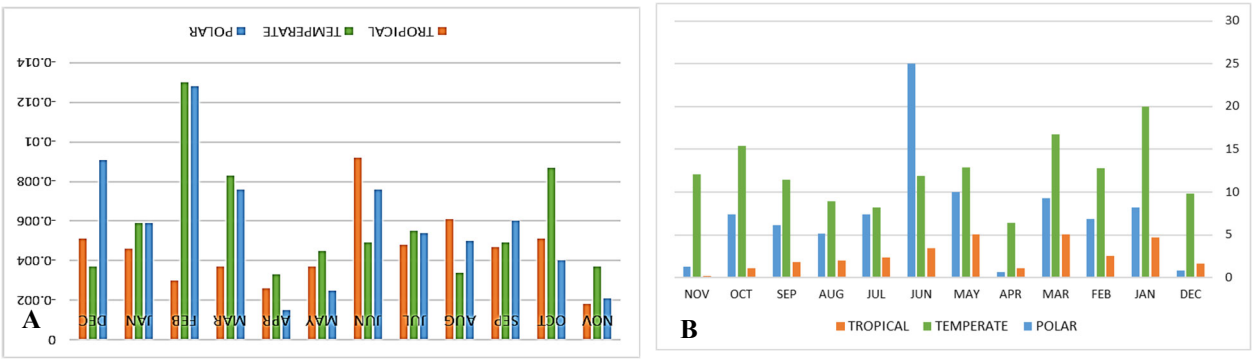

Fig. 9. A – percentage of the area of decreasing trend, B –magnitude of the decreasing trend in the tropical, temperate and polar regions of the Northern Hemisphere during the statistical period of 1994–2023.

3.5. Polar regions

The increasing temperature trend across the entire polar region is clearly evident. *Savita et al*. (2005) attributed the warming of recent decades in the polar region and North America to human activities and internal changes. Seasonal and monthly analyses of the polar region show that the temperature increase is more significant during the cold seasons (*Figs. 4–10, Tables 4* and *5*). However, regional differences in the temperature increase are notable. Although some studies have shown that the highest warming occurs in the high northern latitudes (e.g., *Steiner et al*., 2020), the temperature trend maps in this study indicate that the increase in temperature diminishes between 60 to 90 degrees north and south, with the warming trend decreasing from 60 to 90 degrees north. This finding does not align with *Steiner*'s (2020) results. The discrepancies between our findings and earlier studies, such as *Steiner et al*. (2020), can potentially be attributed to several factors. First, the temporal range of this study (1940–2023) is significantly broader than most previous studies, capturing longer-term climatic trends. Second, differences in datasets this study utilizes, ERA5 reanalysis data may introduce variability due to differing resolutions and calibration techniques. Third, physical changes such as the accelerated melting of the Arctic ice sheets and associated feedback mechanisms, which were less pronounced in earlier studies, could explain the observed divergence. These findings highlight the importance of integrating non-linear models and higher-resolution regional datasets in future research to resolve these contradictions.

Based on these findings, the polar region can be divided into two parts according to the degree of temperature increase, similarly to the tropical region. This division varies by month. In March (*Fig. 5*, A, D), September, October (*Fig. 10*, A, B, D, E), December (*Fig. 4*, A, D), August (*Fig. 8*, C, F), and January (*Fig. 4*, B, E), the temperature increase is greater between 60 to 80 degrees, while the warming decreases between 80 to 90 degrees. In May (*Fig. 5*, C, E), November

(*Fig. 10*, B, E), and April (*Fig. 5*, B, E), the warming is more pronounced between 60 to 75 degrees, while it decreases beyond 75 degrees north. October (*Fig. 10*, B, E) and June (*Fig. 8*, A, D) show the lowest temperature increase in the polar region. In June, from 60 to 90 degrees north, the temperature trend becomes negative, with temperatures dropping between 85 and 90 degrees north (*Fig. 8*, A, D). February exhibits the highest temperature increase in the polar region, with only a slight decrease between 85 to 90 degrees north (*Fig. 4*, B, E). In each of these two parts, regional variations are also notable. For example, Alaska, Siberia, Greenland, and the Arctic Ocean in the subpolar region (up to 75 degrees north) show greater temperature increases compared to latitudes above 75 degrees. This finding contradicts the results of *Stouffer et al.* (1989) and *Manabe et al.* (1991), who suggested that the warming in subpolar regions of the Arctic Ocean is generally minimal. Subpolar oceans have emerged as warming hotspots in the Northern Hemisphere, with higher temperatures than the more northern parts of the polar region. Additionally, cooling cores in the polar regions are located between 60 to 70 degrees north, particularly in southern Greenland, the North Atlantic, Iceland, the Norwegian Sea, and Greenland (again). There are also temperature trend differences between eastern and western parts of the polar region above 70 degrees north, particularly in March, May, June, and July. In May, June, and July, the eastern polar region even experiences a negative temperature trend (*Figs. 4, 5, 8, and 10*). The temperature increase also correlates with the latitude in Greenland, where the warming trend follows a south-to-north gradient. Southern Greenland has the lowest temperature, and as the latitude increases, the warming trend intensifies. *Manabe et al.* (2011) reported a 1 °C temperature decrease in southern Greenland. However, this study found that in October, the opposite occurred, with southern Greenland experiencing higher temperatures, and cooling cores were observed in northern Greenland (*Fig. 10*, B). Alaska and Siberia are warming hotspots in the polar regions. Alaska is a hotspot for increasing temperature trends in North America in every month except September. In September, southern Alaska exhibits a negative trend (*Fig. 10*, A). In December, the temperature increase in Alaska reaches 0.06 °C (*Fig. 4*, A), while in January, it decreases to 0.01 °C (*Fig. 4*, B). The temperature increase in eastern and northern Siberia is also significant. In most months, eastern Siberia serves as a warming core in Europe. During the autumn months, eastern Siberia experiences the highest temperature increase in Europe, reaching up to 0.05 °C (*Fig. 10*). In winter, the increase slows to 0.01 to 0.02 °C (*Fig. 4*). Only in January does eastern Siberia show a negative temperature trend, with a decrease of up to -0.01 °C. The Arctic region has experienced the most significant warming. However, as mentioned at the beginning of this section, this warming decreases as latitudes increase. The annual surface temperature in Alaska and Siberia has increased from 2 °C to 3 °C. Predictions suggest that by 2050, the Arctic region (north of 60 degrees) will warm by 1.1 °C, and by 2100, it could increase by

5.5 °C. The smallest temperature changes are expected in tropical latitudes, with annual variations projected between 0.1 to 3 °C (*Manabe et al*., 2011).

Continents and cold regions of the Northern Hemisphere were analyzed separately. Europe shows a higher warming trend compared to other continents in the Northern Hemisphere. The temperature trend in North Africa closely resembles that of Europe and North America. However, Asia exhibits a different pattern, with a lower warming trend than other continents in most months of the year. Asia shows a lower warming trend compared to Europe, North America, and North Africa (*Figs. 4, 5, 8,* and *10*). Throughout the year, Asia has cooling cores, especially in the tropical and temperate regions, particularly in Pakistan, the southeastern coast of Iran, the Himalayas, and northern, northwestern, and western China. Although studies by *Li* and *Zhang* (2021) for the period 1971–2013 and *Fang et al.* (2016) for the period 1960 to 2010, reported significant warming for most parts of China, and found that warm indices increased faster than cold ones, central China, eastern and northern Tibet, and western China, including the highlands of Xinjiang, have experienced cooling trends throughout the year, making them part of the cooling cores in the Northern Hemisphere. Warming cores in Asia, in all months except November, are mostly concentrated in the Middle East. In November, the warming trend in the Middle East weakens, and even Turkey and Iran experience a cooling trend (*Fig. 10*, C, F). The Arabian Peninsula, which is highly influenced by extreme temperatures (*Krishna,* 2015; *Salimi* and *Al-Ghamdi.,* 2020), and Turkey show a significant warming trend in the Middle East. The Arabian Peninsula, in particular, remains one of the warming cores in the Middle East and Asia throughout the year. Studies by *Paeth et al*. (2009) and *El Kenawy et al*. (2015) have also highlighted significant warming in North Africa and the Middle East.

In *Fig. 10*, autumn temperature trends reveal a gradual warming from tropical to polar regions. Notable variations include consistent warming in September and localized cooling in northern regions during November.

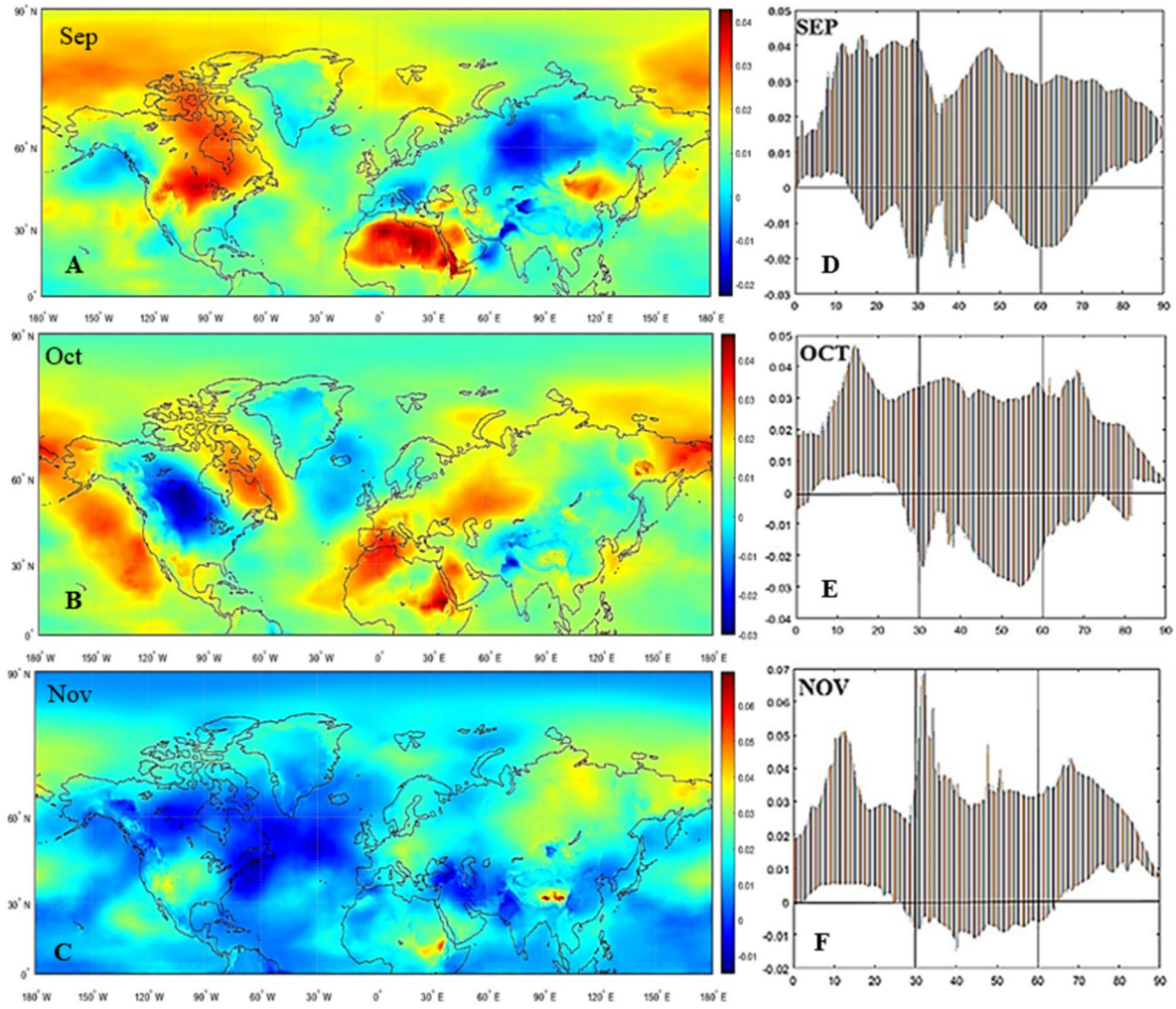

Fig. 10. the temperature trend of the months of September, October, and November in the Northern Hemisphere during the statistical period of 1940–2023.

The Tibetan Plateau, a key warming core in Asia, experiences a warming trend of 0.03 to 0.05 °C annually, with the highest trends (0.07 °C) in the eastern regions during the cold seasons (September to March) (*Figs. 4* and *10*). In contrast, the warming trend during the warm seasons drops to 0.01 °C in August. Over the past 119 years, the extent of cold regions in the Tibetan Plateau has decreased significantly (*Huang*, 2020). Similarly, studies by *Zhang* and *Zhou* (2009), *Zhang et al.* (2013), and *Li* and *Zhang* (2021) confirm these seasonal variations.

South Asia, including the Indian subcontinent, Bangladesh, and Myanmar, shows a weaker warming trend during winter (December to March), with a negative trend of -0.005 °C in February (*Fig. 4*, B). However, in months like August, September, and November, the warming trend intensifies, aligning with *Naveendrakumar et al*. (2019), who reported a linear temperature increase in South Asia.

Cold and high-altitude regions like the Atlas Mountains, Rockies, Alps, Himalayas, and Siberia also exhibit notable trends. The Rockies show warming on western slopes and cooling on eastern slopes during October, with slight cooling in December (*Fig. 4*, A). The Alps, as one of Europe's warming cores, exhibit consistent warming throughout the year, with impacts such as glacier retreat, reduced snow cover below 1300 m, and vegetation shifts (*Paul et al.*, 2004; *Scherrer et al.*, 2004). The Himalayas show warming from August to March and cooling from April to July, with western regions experiencing more significant cooling (*Figs. 5* and *8*). The Atlas Mountains, in contrast, display year-round warming, except in September, where trends drop to 0–0.005 °C (*Fig. 10*, A).

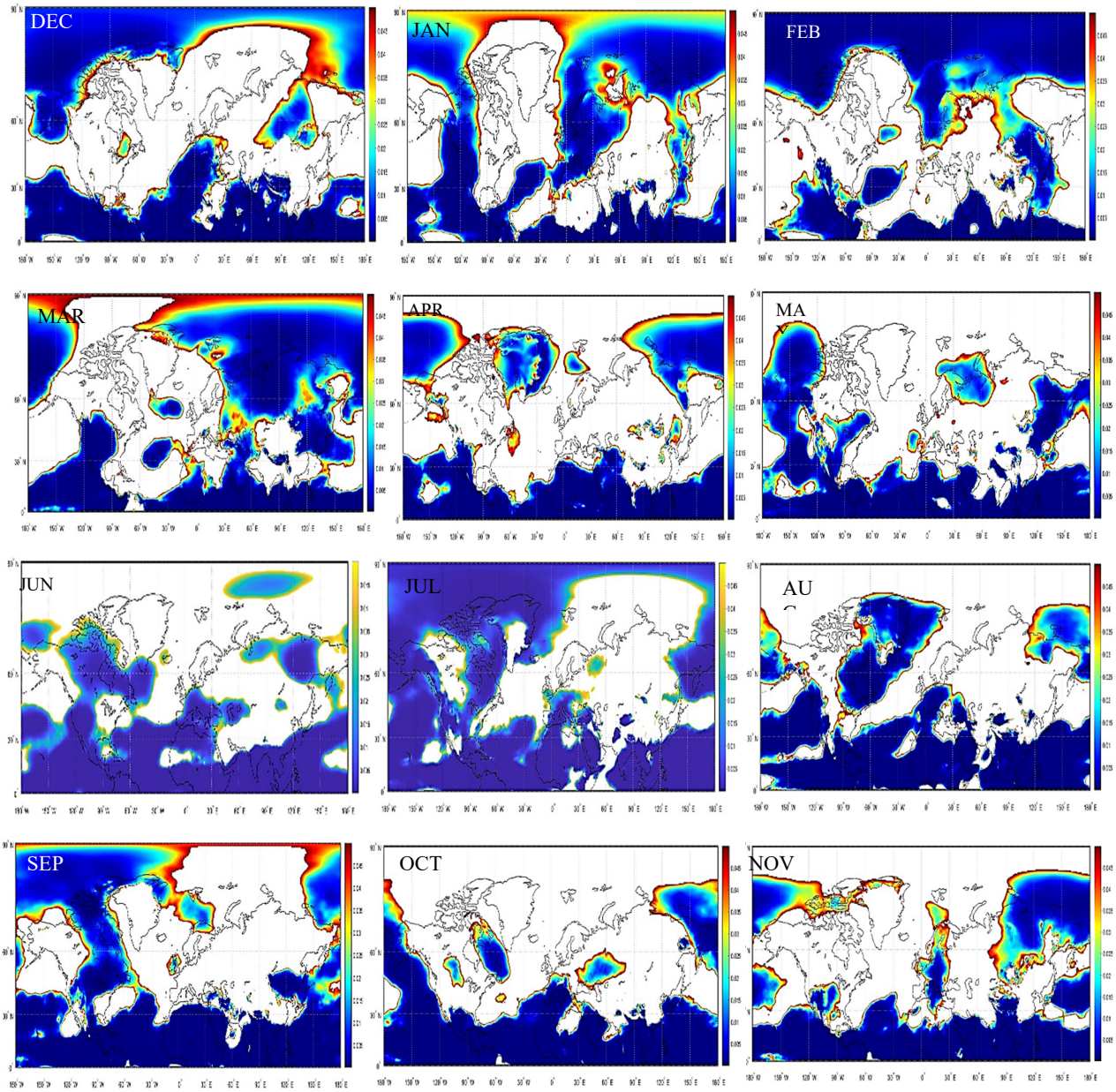

Fig. 11. The significant level of the temperature trend in the Northern Hemisphere during the statistical period of 1940–2023.

Fig. 11 provides a detailed visualization of the spatial and seasonal variability of temperature trends across the Northern Hemisphere during the statistical period of 1940–2023. The figure highlights significant warming in polar regions during winter, particularly in January and February, where trends exceed 0.02 °C per decade. Conversely, the summer months, such as June, exhibit localized areas of decreasing trends, most notably in the tropical and temperate zones. Temperate regions demonstrate marked variability, with pronounced warming during spring and autumn, reflecting the influence of transitional seasonal dynamics. Tropical regions, in contrast, show relatively stable trends with minimal seasonal fluctuations (*Fig. 11*).

4. Conclusion

This study analyzed monthly and seasonal temperature trends in the Northern Hemisphere from 1940 to 2023 using least squares regression at a 95% significance level. Trends were evaluated across the tropical, temperate, and polar regions to examine the intensity and spatial variability of warming and cooling patterns.

The findings revealed that increasing temperature trends dominate all months in the Northern Hemisphere, with evident regional and seasonal variability. The largest area with increasing trends was observed during autumn, while the highest temperature rise occurred in winter. In contrast, summer exhibited the smallest area with increasing trends and the lowest temperature rise. Notably, decreasing trends were most prominent in June, but their intensity did not align consistently with warm or cold months. Conversely, increasing trends were more pronounced in cold months than in warm months.

The analysis highlighted the importance of latitude in shaping warming trends. For instance, while the tropical region exhibited lower overall warming compared to the temperate and polar zones, significant variability was observed within the tropics. Latitudes 0–8°N showed uniform, lower warming, while latitudes 8–30°N exhibited higher warming rates, comparable to the temperate and polar regions. In September, warming in the 8–30°N range even exceeded that in the temperate and polar regions. This variability underscores the limitations of relying solely on average temperature data and emphasizes the need for temperature maps to capture regional nuances.

In the polar regions, the warming trend was most pronounced in winter but showed notable regional variability. The rate of warming diminished beyond the 60°N latitude, reflecting complex interactions between atmospheric circulation, sea ice albedo feedback, and oceanic heat transport. Similarly to the tropics, the polar region could be divided into two zones based on temperature trends, which varied across months.

Continental analysis showed that Europe experienced the highest warming trends, followed by North America and North Africa. Asia exhibited lower

warming trends overall, with cooling cores in regions such as Pakistan, southeastern Iran, the Himalayas, and northern China. Mountain ranges like the Atlas Mountains, Tibetan Plateau, Alps, Rockies, and Appalachians demonstrated year-round warming trends, with Alaska and Siberia forming major warming cores. However, the Himalayas differed, with a weaker warming trend and seasonal cooling from April to July. From August to March, the Himalayas experienced warming trends, highlighting their distinct climatic behavior compared to other mountain ranges.

Acknowledgements: This work is based upon research funded by Iran National Science Foundation (INSF) under project No.4031542.

References

Almazroui, M, 2020: Changes in temperature trends and extremes over Saudi Arabia for the period 1978–2019. *Adv. Meteorol 2020*(1), 8828521. https://doi.org/10.1155/2020/8828421

Al-Mutairi, M, Labban A, Abdeldym A, and *Abdel Basset H*, 2023: Trend Analysis and Fluctuations of Winter Temperature over Saudi Arabia. *Climate 11*(3), 67. https://doi.org/10.3390/cli11030067

Asakereh, H, 2011: Fundamentals of statistical climatology. Zanjan university publication, 222. (In Persian)

Chapman, W. L and *Walsh J. E*, 1993: Recent variation of sea ice and air temperature in high latitudes. *Bull. Amer. Meteor. Soc., 75*, 33–57. https://doi.org/10.1175/1520-0477(1993)074<0033:RVOSIA>2.0.CO;2

Choi G, Collins D, and *Ren G, 2*009: Changes in means and extreme events of temperature and precipitation in the Asia-Pacific network region, 1955–2007, *Int. J. Climatol*. *29*, 1906–1925. https://doi.org/10.1002/joc.1979

Christy J. R, Norris W. B. Spencer R. W, and *Hnilo J. J,* 2007: Tropospheric temperature change since 1979 from tropical radiosonde and satellite measurements. *J. Geophys Res: Atmospheres*, *112*(D6). https://doi.org/10.1029/2005JD006881

Chung Y.S and *Yoon M.B,* 2000: Interpretation of recent temperature and precipitation trends observed in Korea. *Theor. Appl. Climatol*. *67*, 171–180. https://doi.org/10.1007/s007040070006

Croitoru A.E, Holobace I.H, Lazar C, Moldovan F, and *Imbroavce A,* 2012: Air temperature trend and the impact on winter wheat phenology in Romania. *Climatic Change* 111, 393–410. https://doi.org/10.1007/s10584-011-0133-6

El Kenawy A, López-Moreno J I, McCabe M F, Brunsell N.A, and *Vicente-Serrano S.M,* 2015: Daily Temperature Changes and Variability in ENSEMBLES Regional Models Predictions: Evaluation and Intercomparison for the Ebro Valley (NE Iberia). Atmos. Res. Elsevier BV. http://doi.org/10.1016/j.atmosres.2014.12.007

Fang S, Qi Y, Han G, Li Q, and *Zhou G,* 2016: Changing trends and abrupt features of extreme temperature in mainland China from 1960 to 2010, *Atmosphere 7*(2), 22*;* https://doi.org/10.3390/atmos7020022

Feidas H, Makrogiannis T, and *Bora-Senta E,* 2005: Trend analysis of air temperature time series in Greece and their relationship with circulation using surface and satellite data: 1955–2001. *Theor. Appl Climatol 79*, 185–208. https://doi.org/10.1007/s00704-004-0064-5

Folland C.K, Karl T.P, Christy J.R, Clarke R.A, Gruza G.V, Jouzel J, Mann M.E, Oerlemans J, Salinger M.J, and *Wang S.W,* 2001: Observed climate variability and change. In Chapter 2 of Climate Change 2001; The Scientific Basis, Contribution of Working Group I to the Third Assessment Report of the Intergovernmental Panel on Climate Change (IPCC); *Houghton, J.T., Ding, Y., Griggs, .J., Noguer, M., van der Linden, P.J., Xiaoxu, D*., Eds.; Cambridge University Press: Cambridge, UK, 99–181.

Hansen J, Ruedy R, Sato M, and *Lo K* (2010) Global surface temperature change, *Rev. Geophys*. 48, RG4004-. https://doi.org/10.1029/2010RG000345

Huang Y, Zhang L, Li Y, Ren C, Pan T, Zhang W, and *Liu J,* 2023: Characteristics of the Northern Hemisphere cold regions changes from 1901 to 2019. *Sci. Reports 13*, 3879. https://doi.org/10.1038/s41598-023-30263-1

IPCC. 2007: Summary for policymakers. In Climate Change 2007: The Physical Science Basis.Contribution of Working Group I to the 5th Assessment Report of the Intergovernmental Panel on Climate Change (eds *S. Solomon, D. Qin, M. Manning, Z. Chen, M. Marquis, K. B. Averyt M. Tignor and H. L. Miller*). Cambridge, UK: Cambridge University Press.

IPCC. Climate Change 1995: The Science of Climate Change, *J. T. Houghton et al.,* Eds. Cambridge Univ. Press, Cambridge.

IPCC. Climate change, 2013: The Physical Science Basis. In Contribution of Working Group I to the Fifth Assessment Report of the Intergovernmental Panel on Climate Change; *Stocker, T.F., Qin, D., Plattner, G.K., Tignor, M., Allen, S.K., Boschung, J., Nauels, A., Xia, Y., Bex, V., Midgley, P.M*., Eds.; Cambridge University Press: Cambridge, UK; New York, NY, USA.

IPCC. Climate Change, 2014: Mitigation of Climate Change. In Contribution ofWorking Group III to the Fifth Assessment Report of the Intergovernmental Panel on Climate Change; *Edenhofer, O., Pichs-Madruga, R., Sokona, Y., Farahani, E., Kadner, S., Seyboth, K., Adler, A., Baum, I., Brunner, S., Eickemeier, P., et al*., Eds.; Cambridge University Press: Cambridge, UK; New York, NY, USA.

Jones PD and *Moberg A,* 2003: Hemispheric and large-scale surface air temperature variations: an extensive revision and an update to 2001. *J climate 16*(2):206–223.

Karl TR, Jones PD, Knight RW, Kukla G, Plummer N, Razuvayev V, Gallo KP, Lindseay J, Charlson RJ, and *Peterson TC,* 1993: Asymmetric trends of daily maximum and minimum temperature. *Papers Nat Resour 1*,185. https://doi.org/10.1175/1520-0477(1993)074<1007:ANPORG>2.0.CO;2

Karoly D.J and *Braganza K,* 2005: Attribution of recent temperature changes in the Australian region. *J. Climate 18*, 557–565. https://doi.org/10.1175/JCLI-3265.1

Krzyżewska A, Wereski S, and *Demczuk P,* 2020: Biometeorological conditions during an extreme heatwave event in Poland in August 2015. *Weather 75*(6), 183–189. https://doi.org/10.1002/wea.3497

Li L and *Zhang R,* 2021: Effect of upper-level air temperature changes over the Tibetan Plateau on the genesis frequency of Tibetan Plateau vortices at interannual timescales. *Climate Dynamics 57*(1), 341–352. https://doi.org/10.1007/s00382-021-05715-x

Lindsay, R.W and *Zhang L,* 2005: The thinning of Arctic sea ice, 1988–2003: Have we passed a tipping point? *J. Climat 18*, 4879–4894. https://doi.org/10.1175/JCLI3587.1

Lindzen, R.S and *Giannitsis C*, 2002: Reconciling observations of global temperature change. *Geophys. Res Letters*, *29*(12), 25-1. https://doi.org/10.1029/2001GL014074

Manabe, S and*, Stouffer R.J,* 1980: Sensitivity of a global climate model to an increase of CO2 concentration in the atmosphere. *J. Geophys. Res. 85*, 5529–5555. https://doi.org/10.1029/JC085iC10p05529

Manabe, S and*, Stouffer R.J,* 1979: A CO2-climate sensitivity study with a mathematical model of the global climate. *Nature 282*, 591–593. https://doi.org/10.1038/282491a0

Manabe S,Stouffer R,J, Spelman K, and *Bryan K,* 1991: Transient response of a coupled ocean–atmosphere model to gradual changes of atmosphericCO2. Part I: Annual mean response. *J. Climate 5*, 785–818. https://doi.org/10.1175/1520-0442(1991)004<0785:TROACO>2.0.CO;2

Manabe S., Ploshay J, and *Lau N. C,* 2011: Seasonal variation of surface temperature change during the last several decades. *J. Climate 25*, 3817–3821. https://doi.org/10.1175/JCLI-D-11-00129.1

Momeni, M, 2008: Statistical analysis using Spss software. New book publication, 35. (in Persian)

Naveendrakumar G, Vithanage M, Kwon HH, Chandrasekara SS, Iqbal MC, Pathmarajah S, Fernando WC, and *Obeysekera J,* 2019: South Asian perspective on temperature and rainfall extremes: a review, *Atmos. Res*. *225*, 110–120. https://doi.org/10.1016/j.atmosres.2019.03.021

Neter J, Wasserman W, and *Whitmore G.A,* 1988: Applied Statistics. Third Edition, Allyn and Bacon, Inc, 820–822.

Otterman J, Angell J.K, Ardizzone J, Atlas R, Schubert S, Starr D, and *Wu, M.L,* 2002: North-Atlantic surface winds examined as the source of winter warming in Europe. *Geophys. Res. Lett 29*, 18. https://doi.org/10.1029/2002GL015256

Paeth H, Born K, Girme, R, Podzun R, and *Jacob D,* 2009: Regional Climate Change in Tropical and Northern Africa due to Greenhouse Forcing and Land Use Changes. *J. Climate 22*, 115–132. https://doi.org/10.1175/2008JCLI2390.1

Paul F, Kääb A, Maisch M, Kellenberger T, and *Haeberli W,* 2004: Rapid disintegration of Alpine glaciers observed with satellite data. Geophys. *Res. Lett. 31*(21). https://doi.org/10.1029/2004GL020816

Quintana-Gomez R.A, 1999: Trends of maximum and minimum temperatures in Northern South America. *J. Climate 12*, 2105–2112. https://doi.org/10.1175/1520-0442(1999)012<2104:TOMAMT>2.0.CO;2

Reidmiller D.R, Avery C.W, Easterling D.R, Kunkel K.E, Lewis K.L.M, Maycock T.K, and *Stewart B.C,* 2018: Fourth national climate assessment, Volume II: Impacts, risks, and adaptation in the United States. Washington, DC, US Global Change Research Program.

Rosenzweig C, Karoly D, Vicarelli M, Neofotis P, Wu Q, Casassa G, Menzel A, Root T.L, Estrella N, Seguin B, and *Tryjanowski P,* 2008: Attributing physical and biological impacts to anthropogenic climate change, *Nature, 453*(7193), 353–357. https://doi.org/10.1038/nature06937

Salimi M and *Al-Ghamdi S.G,* 2020: Climate change impacts on critical urban infrastructure and urban resiliency strategies for the Middle East, *Sust. Cities Soc. 55,* 101958. https://doi.org/10.1016/j.scs.2019.101948

Salinger, M.J, 2005: Climate variability and change: past, present and future–an overview. *Climatic*

Savita A, Kjellsson J. J, Latif M, Nnamchi, H, and *Wahl, S*, 2025: Impact of multidecadal climate'modes variability on the Northern Hemisphere temperature trend in the recent decades (No. EGU25-11758). Copernicus Meetings. https://doi.org/10.5194/egusphere-egu24-11748

Scherrer SC, Appenzeller C, and *Laternser M,* 2004: Trends in Swiss Alpine snow days: The role of local- and large-scale climate variability. *Geophys Res Lett 31*, L13215. https://doi.org/10.1029/2004GL020255

Seidel D. J, Fu ., Randel W. J, and *Reichler, T.J*, 2008: Widening of the tropical belt in a changing climate. *Nat. Geosci. 1*, 21–25. https://doi.org/10.1038/ngeo.2007.38

Siddik. M and *Rahman. M,* 2014: Trend analysis of maximum, minimum, and average temperatures in Bangladesh: 1961–2008, *Theor Appl Climatol 116*(3–4). https://doi.org/10.1007/s00704-014-1135-x

Simmons A. J, Berrisford P, Dee D. P, Hersbach H, Hirahara S, and *Thépaut J.-N,* 2017: A reassessment of temperature variations and trends from global reanalyses and monthly surface climatological datasets, *Quart J Roy Meteorol Soc 153*(702), 101–119. https://doi.org/10.1002/qj.2949

Steiner AK, Ladstädter F, Randel WJ, Maycock AC, Fu Q, Claud C, Gleisner H, Haimberger L, Ho SP, Keckhut P, and *Leblanc T,* 2020: Observed temperature changes in the troposphere and stratosphere from 1979 to 2018. *J. Climate 33*(19):8165–8194. https://doi.org/10.1175/JCLI-D-19-0998.1

Stouffer R. J, Manabe S, and *Bryan K,* 1989: Interhemispheric asymmetry in climate response to a gradual increase of atmospheric CO2. *Nature 352*, 660–662.https://doi.org/10.1038/342660a0

Tamarin-Brodsky T, Hodges K, Hoskins B. J, and *Shepherd T.G,* 2019: A dynamical perspective on atmospheric temperature variability and its response to climate change. *J. Climate 32*, 1707–1725. https://doi.org/10.1175/JCLI-D-18-0462.1

Trewin L. V, 2016: Global observed long-term changes in temperature and precipitation extremes: a review of progress and limitations in IPCC assessments and beyond, *Weather Climate Extremes 11*, 5–16. https://doi.org/10.1016/j.wace.2015.10.007

Vinnikov K.Y, Groisman P.Y, and *Lugina K.M,* 1990: Empirical Data on Contemporary Global Climate Changes (Temperature and Precipitation). *J. Climate 3*, 662–677. https://doi.org/10.1175/1520-0442(1990)003<0662:EDOCGC>2.0.CO;2

Zhang D, Huang J, Guan X, Chen B, and *Zhang L,* 2013: Long-term trends of precipitable water and precipitation over the Tibetan Plateau derived from satellite and surface measurements. Journal of Quantitative Spectroscopy *Radiative Transfer 122,* 64–71. https://doi.org/10.1016/j.jqsrt.2012.11.028

Zhang RH and *Zhou SW,* 2009: Air temperature changes over the Tibetan Plateau and other regions in the same latitudes and the role of ozone depletion. *Acta Meteorol Sin 23*, 290–299.